Pre-print of published paper:
To cite this article: Tajeripour, F., & Fekri-Ershad, S. (2014). Developing a novel approach for stone porosity computing using modified local binary patterns and single scale retinex. *Arabian Journal for Science and Engineering, 39*(2), 875-889.
DOI 10.1007/s13369-013-0725-8

Developing a Novel Approach for Stone Porosity Computing Using Modified Local Binary Patterns and Single Scale Retinex

Farshad Tajeripour[1], Shervan Fekri Ershad[2]

[1.2.] Faculty of Electrical and Computer engineering,
Shiraz University, Shiraz, Iran
[1.] tajeri@shirazu.ac.ir [2.] shfekri@shirazu.ac.ir

Abstract:

Defect detection is one of the problems which has been paid much attention on by image processing scientists since late 90s. Since now many different methods have been proposed to defect detection based on texture analysis. According to surface defect description, stone porosity can be categorized as a defect. An approach which provides discriminant features for texture analysis is two dimensional local binary patterns. In this paper for the first time, a method is proposed for detecting abnormalities in stone textures based on one dimensional local binary patterns. The proposed approach includes two stages. First of all, in training stage, one dimensional local binary pattern is applied on full porosity-less stone images and the basic feature vector is calculated. Then, by image windowing and computing the non-similarity amount between these windows and basic vector, a threshold is computed for porosity-less stones. Finally, in testing stage, by using the porosity-less threshold the porosities are detected on test images. Also, another stage is proposed for normalization stone images based on single scale retinex algorithm. By using image normalization, the detection accuracy of proposed approach is improved. High detection rate, low computational complexity, and noise insensitivity are advantages of the proposed approach. The proposed approach is fully automatic and all of the necessary parameters can be tuned. Also, the proposed approach can be used for every case of defect detections.

Keywords:

Porosity, Defect Detection, feature extraction, Local Binary Pattern, Single Scale Retinex, Logarithm Likelihood

Pre-print of published paper:
To cite this article: Tajeripour, F., & Fekri-Ershad, S. (2014). Developing a novel approach for stone porosity computing using modified local binary patterns and single scale retinex. *Arabian Journal for Science and Engineering, 39*(2), 875-889.
DOI 10.1007/s13369-013-0725-8

Developing a Novel Approach for Stone Porosity Computing Using Modified Local Binary Patterns and Single Scale Retinex

1. Introduction:

Any hole, damage and slot in stones are called porosity. The porosity amount is an important factor for architectonic stones, because the quality of structure is dependent to the porosity amount. Also, the strength of structure or building against earthquake and torrent is dependent to the porosity amount. In the Civil literature, the porosity amount is computed by Eq.1.

$$\text{Porosity Amount} = \frac{\text{P.A}(\text{m}^2)}{\text{S.A}\ (\text{m}^2)} * 100 \qquad (1)$$

Where, P.A means the porosity area and S.A is full stone area. So porosity amount is percental. Some examples of porosity are shown in Fig.1.
In stonecutting factories, one of the basic features for categorization the quality of stones is its porosity amount. Now, in near all of the stonecutting factories, the porosity amount is computed by experts. So, it's necessary to propose a visual inspection approach to decrease time and costs and increase detection accuracy. According to stone images and surface defect description, porosity can be categorized as defect. So, the defect detection algorithms can be used for detecting stone porosities.

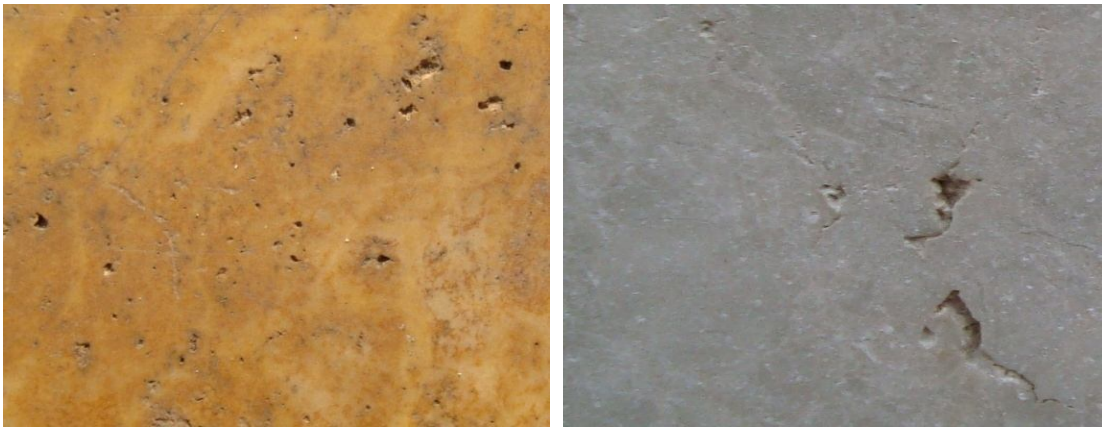

(a) (b)
Figure 1. example of porosity (a) orange travertine (b) Harsin Marble

Consequently, since now, many different approaches are proposed for defect detection in various applications. For example, Zhaoa and Yeb [1] are proposed an approach for wood defect detection recognition. In [2] the authors offered an accurate method for ceramic tiles visual inspection system. In [3], [4] and [5] some defect detection approaches are proposed for cases such as leather, fabric textile and boiler.
In [6] the techniques used to texture analysis and defect detection are discussed in four categories, statistical approaches, Structural approaches filter based methods, and model based approaches. Table 1 shows a summary list of some of the key texture analysis methods that have been developed for texture analyzing. Clearly, statistical and filter based approaches are very popular.
Statistical texture analysis methods measure the spatial distribution of pixel values. They are well rooted in the computer vision world and have been extensively applied to various tasks. A large number of statistical texture features have been proposed, ranging from first order statistics to higher order statistics. Amongst many, histogram statistics [7], co-occurrence matrices [8], local binary patterns [9] and autocorrelation [11] have been applied to texture Analysis. In structural approaches, texture is characterized by texture primitives or texture elements, and the spatial arrangement of these

Pre-print of published paper:
To cite this article: Tajeripour, F., & Fekri-Ershad, S. (2014). Developing a novel approach for stone porosity computing using modified local binary patterns and single scale retinex. *Arabian Journal for Science and Engineering*, *39*(2), 875-889.
DOI 10.1007/s13369-013-0725-8

primitives. Thus, the primary goals of structural approaches are firstly to extract texture primitives, and secondly to model or generalize the spatial placement rules. The texture primitive can be as simple as individual pixels, a region with uniform gray levels, or line segments. The placement rules can be obtained through modeling geometric relationships between primitives or learning statistical properties from texture primitives. The filter based techniques largely share a common characteristic, which is applying filter banks on the image and compute the energy of the filter responses. The methods can be divided into spatial domain [17], frequency domain [18], and joint spatial/spatial-frequency domain techniques [19]. Model based methods include, among many others, fractal models [20], random field models [21], texem model [22], epitome model [23], and autoregressive models [24].

Category	Method
Statistical	1. Histogram properties [7] 2. Co-occurrence matrix [8] 3. Local binary pattern [9] 4. Other gray level statistics [10] 5. Autocorrelation [11] 6. Registration-based [12]
Structural	1. Primitive measurement [13] 2. Edge Features [14] 3. Skeleton representation [15] 4. Morphological operations [16]
Filter Based	1. Spatial domain filtering [17] 2. Frequency domain analysis [18] 3. Joint spatial/spatial-frequency [19]
Model Based	1. Fractal models [20] 2. Random field model [21] 3. Texem model [22] 4. Epitome model[23] 5. Autoregressive [24]

Table 1: Inexhaustive list of textural analysis methods

According to our researches, since now, no approach is developed for porosity detection on stones. Local binary pattern (LBP) is an operator for computing local contrast of each pixel. It's first proposed by Ojala et al in [25]. And the improved version of that is offered in [27] which is a two dimensional operator. In this paper first of all, a new version of LBP is proposed based on one dimensional modified local binary patterns for detecting stone porosities. Next, a novel approach is proposed for computation stone porosity based on one dimensional LBP. The proposed approach includes two stages. The first stage is training. In this stage, some surely porosity-less images were taken and analyzed by one dimensional local binary pattern operator and a basic feature vector is computed, Which is a good identification for non-porosity images. After that, by using image windowing technique and Log-Likelihood ratio, an accurate threshold is computed for porosity-less. The second stage is testing. In this, by extracting modified local binary pattern features of test images and compared them with basic vector, porosity parts are detected. Also, to increase quality of our porosity detection approach, another stage is proposed based on single scale retinex technique as preprocessing stage. In this stage, by using Gaussian function, images are normalized. In the result part, some of stone images are captured and the proposed approach applied on them. High detection rate shows the quality of the proposed approach. Low computation complexity, rotation invariant, noise insensitivity and illumination invariant, are some of other advantages. Also, the porosity detection approach is applied on database based on previous two dimensional LBP.

1.1 Paper organization:

Pre-print of published paper:
To cite this article: Tajeripour, F., & Fekri-Ershad, S. (2014). Developing a novel approach for stone porosity computing using modified local binary patterns and single scale retinex. *Arabian Journal for Science and Engineering, 39*(2), 875-889.
DOI 10.1007/s13369-013-0725-8

This paper is organized as follows: Section two is related to the basic version of Local binary patterns. Section three is related to the description of improved version of Local binary pattern in two dimensional. In section four, the proposed one dimensional local binary pattern operator is described. In Section five the proposed approach for detecting the stone porosity is described. In section six, an image normalization algorithm is offered based on single scale retinex. Finally, experimental results are presented in sections 7. Also, in section8, the proposed approach for stone quality categorization is offered.

2. Local Binary Patterns:

The local binary patterns (LBP) is a non-parametric operator which describes the local spatial structure and local contrast of an image. Ojala et al. [25] first introduced this operator and showed its high discriminative power for texture classification.

At a given pixel position (x_c, y_c), LBP is defined as an ordered set of binary comparisons of pixel intensities between the center pixel and its surrounding pixels. Usually to achieve the rotation invariant, neighborhoods would be assumed circular. So, points which the coordination's are not exactly located at the center of pixel would be found by interpolation. Some of the circular neighborhoods by radius(R) and (P) neighborhoods pixels are shown in Fig.2.

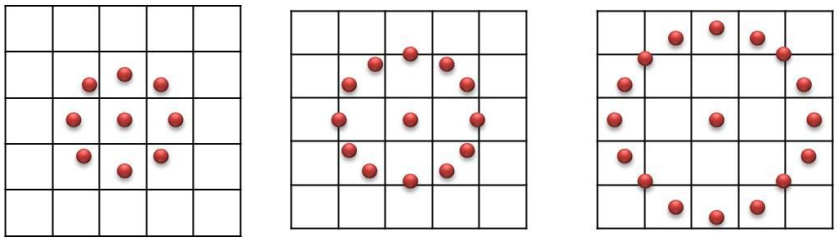

(a) (b) (c)

Figure(2). Some examples of circular neighborhoods
(a) P=8 R=1 (b) P=12 R=1.5 (c) P=16 R=2

Now, the local binary patterns are defined at a neighborhood of image by Eq.2.

$$LBP_{P,R} = \sum_{n=0}^{p-1} s(g_n - g_c)2^n \qquad (2)$$

Where, "g_c" corresponds to the grey value of the centered pixel and "g_n" to the grey values of the neighborhood pixels. Also, P is the number of neighborhoods of center pixel, and function s(x) is defined as:

$$s(x) = \begin{cases} 1 & \text{if } x \geq 0 \\ 0 & \text{if } x < 0 \end{cases} \qquad (3)$$

2.1. Achieving Rotation invariance

According to [25], The $LBP_{P,R}$ operator produces (2^P) different output values, corresponding to the 2^P different binary patterns that can be formed by the P pixels in the neighbor set. When the image is rotated, the gray values g_n will correspondingly move along the perimeter of the circle around g_c. To remove the effect of rotation, i.e. to assign a unique identifier to each rotation invariant local binary patterns is defined:

$$LBP^{ri}_{P,R} = \min\{ROR\{LBP_{P,R}, \alpha) \mid \alpha = 0,1, \dots, p-1\} \qquad (4)$$

Where "ri" correspond to rotation invariant and ROR(x, α) performs a circular bit-wise rotate right on the P-bit number x, α times. Finally, the minimum of computed values for α=0 to p-1 would be choose.

3. Two Dimensional Local binary patterns

The author's practical experience in [26], showed that computation complexity of basic local binary patterns is too high. To solve this, Ojala et al [27] defined an uniformity measure "U", which

Pre-print of published paper:
To cite this article: Tajeripour, F., & Fekri-Ershad, S. (2014). Developing a novel approach for stone porosity computing using modified local binary patterns and single scale retinex. *Arabian Journal for Science and Engineering, 39*(2), 875-889.
DOI 10.1007/s13369-013-0725-8

corresponds to the number of spatial transitions (bitwise 0/1 changes) in the "pattern". It is shown in Eq.5. For example, patterns 00000000 and 11111111 have U value of 0, while 00011101 have U value of 3.

$$U(LBP_{P,R}) = |s(g_{p-1} - g_c) - s(g_0 - g_c)| + \sum_{i=1}^{p-1} |s(g_i - g_c) - s(g_{i-1} - g_c)| \quad (5)$$

In this version of LBP, the patterns which have uniformity amount less than U_T are categorized as uniform patterns and the patterns with uniformity amount more than U_T categorized as non-uniform patterns. Finally, the LBP is computed by using Eq.6.

$$LBP_{P,R}^{riu_T} = \begin{cases} \sum_{i=0}^{P-1} s(g_i - g_c) & \text{if } U(LBP_{P,R}) \le U_T \\ P + 1 & \text{otherwise} \end{cases} \quad (6)$$

Superscript "riu_T" reflects the use of rotation invariant "uniform" patterns that have U value of at most U_T.

According to Eq.6, applying LBP will assign a label from 0 to P to uniform patterns and label P+1 to non-uniform patterns.

Because, in this version of LBP just one label (P+1) is assigned to all of the non-uniform patterns, so uniform labels should cover mostly patterns in the image. In [28], Tajeripour et al show that if in the definition of LBP operator the value of U_T is selected equal to (P/4), only a negligible portion of the patterns in the texture takes label P+1.

According to selecting two dimensional neighbors, the improved version of local binary patterns is a two dimensional operator. So, it causes much computation complexity for inspection systems. In the next section, one dimensional LBP is proposed to decrease the computation complexity and increase the accuracy rate of texture analyzing and classification.

4. Proposed One Dimensional Local Binary Patterns

In the basic (section 2) and improved version of LBP operator (section3) selecting neighborhood in circular form is to make the algorithm invariant to rotation. Since during inspection process, selecting circular neighborhood is not necessary. Also, computing brightness using interpolation in circular neighborhood needs a large amount of computations. Therefore, in this version of LBP, the neighborhood is a row (column) wise line segment.

In order to apply one dimensional LBP, the gray value of the first pixel in the segment is compared with gray value of other pixels in the segment. Fig.3 describes how to apply the one dimensional LBP operator on a sample column segment.

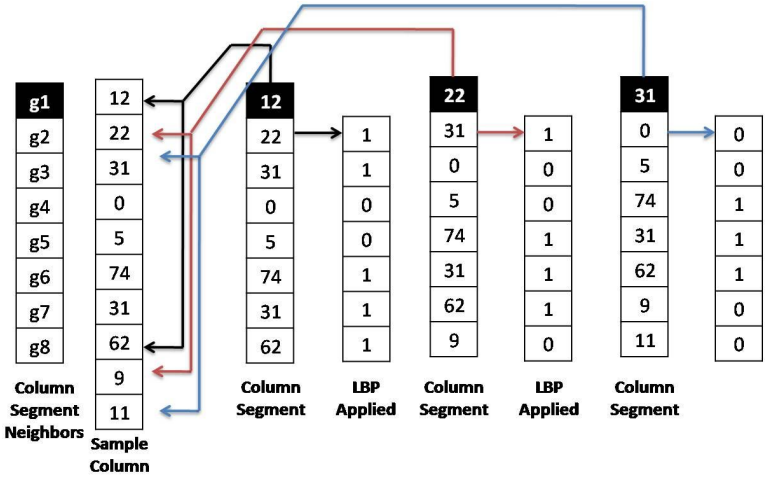

Figure (3). Applying LBP on a sample row of image with a segment of length 8 pixels

Pre-print of published paper:
To cite this article: Tajeripour, F., & Fekri-Ershad, S. (2014). Developing a novel approach for stone porosity computing using modified local binary patterns and single scale retinex. *Arabian Journal for Science and Engineering, 39*(2), 875-889.
DOI 10.1007/s13369-013-0725-8

In this version of LBP, the uniformity measure "U" corresponds to the number of spatial transitions (bitwise 0/1 changes) in the row (column) segment (Eq.7).

$$U(LBP_L) = |s(g_L - g_1) - s(g_2 - g_1)| + \sum_{i=2}^{L-1} |s(g_i - g_1) - s(g_{i+1} - g_1)| \qquad (7)$$

Where g_i represents the intensity of the i_{th} neighbors and g_1 is the intensity of the first pixel of each row (column) segment. Also, L is the size of row (column) segments, so the notation of Local binary patterns is renamed from $LBP_{P,R}$ to LBP_L.

In one dimensional local binary patterns, row (column) segments that have uniformity amount less than uniformity threshold are categorized as uniform segments and row (column) segments that have uniformity amount more than uniformity threshold are categorized as non-uniform segments. So, the local binary patterns is measured by using Eq.8.

$$LBP_L^{U_T} = \begin{cases} \sum_{i=2}^{L} S(g_i - g_1) & \text{if } U(LBP_L) \le U_T \\ L & \text{Otherwise} \end{cases} \qquad (8)$$

According to Eq.8, if the length of the row (column) segment is considered L pixels, applying LBP will assign a label from 0 to L-1 to uniform segments and label L to non-uniform segments.

Because, in one dimensional LBP just one label (L) is assigned to all of the non-uniform segments, so uniform labels should cover mostly segments. In [28], Tajeripour et al show that if in the definition of LBP operator the value of U_T is selected equal to (L/4), only a negligible portion of the patterns in the texture takes label L.

According to selecting row (column) segments as neighbors, this version of local binary patterns is a one dimensional operator. So, its computation complexity is less than two dimensional local binary patterns.

4.1. Feature Extraction

As it was explained in previous section, a label is assigned to each row (column) segment. Regarding the Eq.8, if the length of each row (column) segment considered "L" pixels, applying LBP_L will assign a label from zero to "L-1" to uniform segments and label "L" to non-uniform segments. So, for every image, two "L+1" dimensional feature vector can be extracted.

To extract the feature vector, first the LBP_L is applied on the image and the labels are assigned to row (column) segments. Then the occurrence probability of each label in the image is regarded as one of the dimensions of the feature vector. The occurrence probability of a specific label in the image can be approximated by the ratio of the number of that label to the number of all labels (Eq.9).

$$P_i = \frac{N_{P_i}}{N_{total}} \qquad 0 \le i \le L \qquad (9)$$

Where, N_{p_i} is the number of row (column) segments that labeled as P_i, and N_{total} is the number of all row (column) segments. The feature extraction can be done once for the row segments and once for the column segments. So, for every image, two "L+1" dimensional feature vector can be extracted. The extracted feature vector for row (column) segments is shown in Eq.10.

$$R_x = < p_0, p_1, \ldots, p_L > \qquad (10)$$

Where, R_x is the feature vector extracted for row segmentations and there is a same way for R_y.

5. Proposed Porosity Detection Approach

Any hole, damage and slot in stones are called porosity. In this section, a novel approach is proposed for detecting porosities in architectonic stones. The proposed approach is consisting of a training stage and a testing stage.

5.1. Training Stage

In the training stage, first an image is taken from the stone which is porosity-less. Then one dimensional LBP is applied over the whole image. After that, regarding the Eq.10, two feature vectors

Pre-print of published paper:
To cite this article: Tajeripour, F., & Fekri-Ershad, S. (2014). Developing a novel approach for stone porosity computing using modified local binary patterns and single scale retinex. *Arabian Journal for Science and Engineering, 39*(2), 875-889.
DOI 10.1007/s13369-013-0725-8

are extracted from it. These vectors are called Basic feature vectors for rows and columns, and are denoted by "M_x" and "M_y".

Then the porosity-less image is divided into windows of sizes W×W pixels. After that, the one dimensional LBP is applied over each of these windows. Thus, for each window, a feature vector is extracted.

Then, the non-similarity amount of the rows (columns) vector in each window is computed through the basic rows (columns) feature vector based on Log-likelihood ratio (Eq.11, Eq.12).

Since minimization of Log-likelihood ratio shows the similarity to specific class. So, the maximum value among these ratios is regarded as the threshold for the porosity-less window (Eq.13, Eq.14).

$$\mathbf{L_{xk}} = (S_{xk}, M_x) = \sum_{i=1}^{L+1} S_{iyk} \log\left(\frac{S_{ixk}}{M_{xi}}\right) \quad k = 1,2,\dots,N \qquad (11)$$

$$\mathbf{L_{yk}} = (S_{yk}, M_y) = \sum_{i=1}^{L+1} S_{ixk} \log\left(\frac{S_{iyk}}{M_{yi}}\right) \quad k = 1,2,\dots,N \qquad (12)$$

Where "S_{xk}" and "S_{yk}"is the feature vectors which extracted for "K_{th}" window in row wise and column wise. M_x and M_y are the basic feature vectors. Also, N is the number of windows and "i" represents the "i_{th}" dimension of the feature vector.

$$\mathbf{T_x} = \max(L_{xk}) \quad k = 1,2,\dots,N \qquad (13)$$

$$\mathbf{T_y} = \max(L_{yk}) \quad k = 1,2,\dots,N \qquad (14)$$

Where, "T_x" and "T_y" are the non-porosity thresholds (porosity-less threshold) in row and column segments. "L_k" shows the non-similarity amount between "K_{th}" and Basic vector. The flowchart of the training stage is shown in Fig.4.

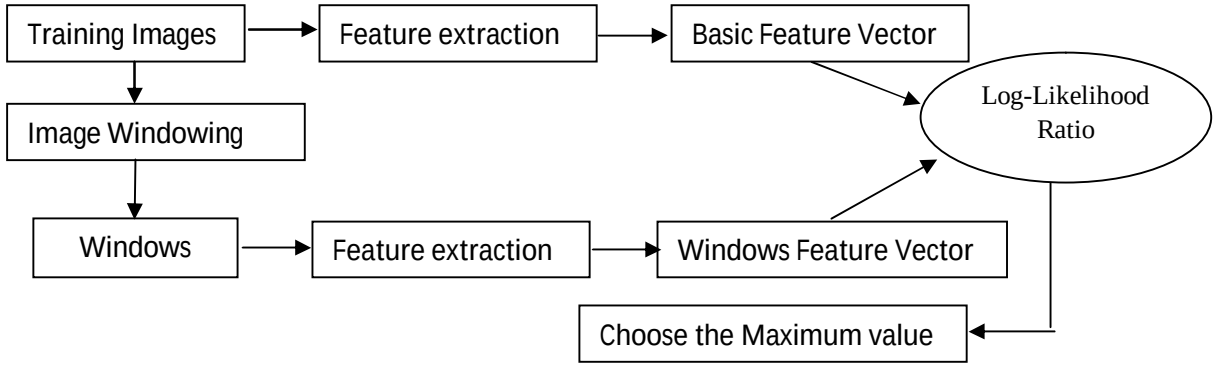

Figure4. The flowchart of Train Stage

5.2. Testing Stage

In the testing stage, first the test image is divided into windows of sizes W×W pixels. Then, for each window, the rows (column) feature vector is extracted. After that, for each of these windows the log-likelihood ratio is computed (Eq.15, Eq.16).

The detection rate of proposed approach is related to the size of windows. There are two important points to determining the optimum size of windows as following:

I) The larger the size of windows considered, the more accurate values would be obtained for feature vectors which are extracted for that window. But the larger the size of windows considered the detection rate would decrease for small porosities.

II) The numbers of operators which are applied on each window are related to the size of window and the length of row (column) segments. In [28], the authors suggest that the number of applied operators must be larger than a threshold. If the size of windows be W×W and the length of segments be L pixels, so the number of operators that are applied on each window is equal to "W× (W-L+1)". For example, if operators number considered to be 100, consequently "$W^2 – W (L - 1) - 100 > 0$ ".

Pre-print of published paper:
To cite this article: Tajeripour, F., & Fekri-Ershad, S. (2014). Developing a novel approach for stone porosity computing using modified local binary patterns and single scale retinex. *Arabian Journal for Science and Engineering, 39*(2), 875-889.
DOI 10.1007/s13369-013-0725-8

For each window, if any of these ratios is greater than the corresponding threshold, the window is declared as the porous window. It is shown in Eq.17.

$$\mathbf{D_{xk}} = (R_{xk}, M_x) = \sum_{i=1}^{L+1} R_{ixk} \log\left(\frac{R_{ixk}}{M_{xi}}\right) \quad k = 1,2,\dots,N \qquad (15)$$

$$\mathbf{D_{yk}} = (R_{yk}, M_y) = \sum_{i=1}^{L+1} R_{iyk} \log\left(\frac{R_{iyk}}{M_{yi}}\right) \quad k = 1,2,\dots,N \qquad (16)$$

Where "R_k" is the feature vector of row (column) process which is computed for "K_{th}" window of testing image. "M_x" and "M_y" are the basic vectors. Also, N is the total number of windows and "i" represents the "i_{th}" dimension of the feature vector. The flowchart of the testing stage is shown in Fig.5.

$$K_{th}\ \text{Window} = \begin{cases} \text{Porous} & \text{if} \quad D_{xk} > T_x \ \text{or}\ D_{yk} > T_y \\ \text{Non} - \text{Porous} & \text{otherwise} \end{cases} \qquad (17)$$

Output of the proposed approach is a binary image which is called defect pattern. Black pixels in the defect pattern represent porosity-less areas of the stone and white pixels represent porous areas.

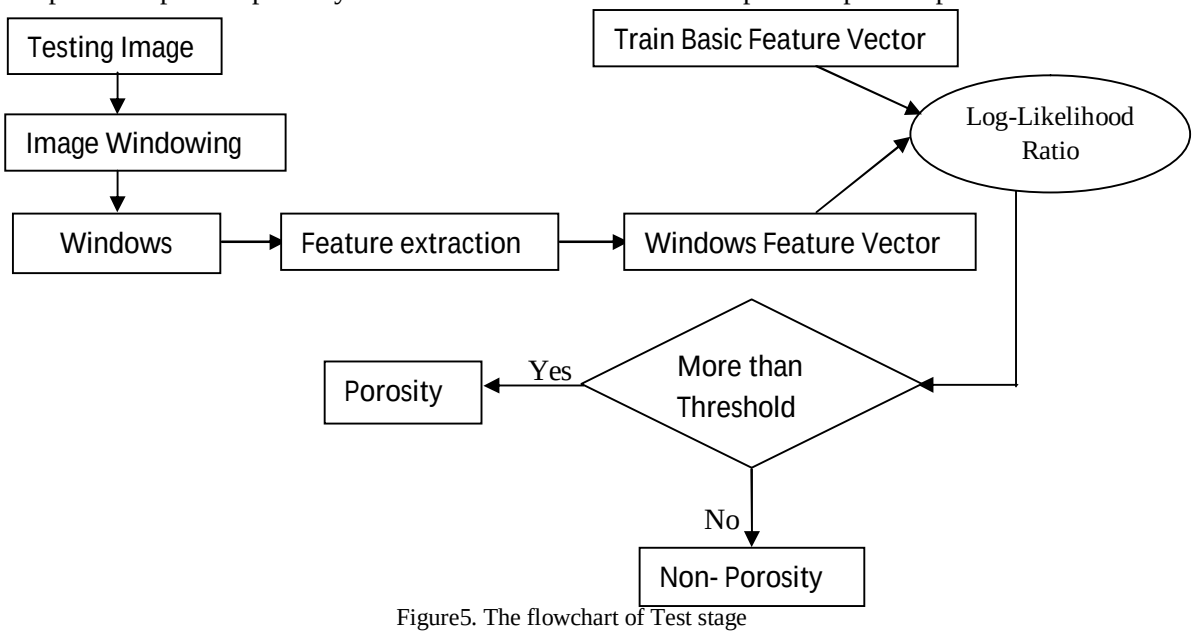

Figure5. The flowchart of Test stage

6. Image Normalization based on SSR

In 1971 Land and McCann [29] introduce the idea that image I(x,y) is the product of two components, illumination L(x, y) and reflectance R(x, y).

$$I(x, y) = L(x, y).R(x, y) \qquad (18)$$

Illumination contains geometric properties of the scene (i.e., the surface normals and the light source position) and reflectance contains information about the object. Based on the assumption that the illumination varies slowly across different locations of the image and the local reflectance may change rapidly across different location, the processed illumination should be drastically reduced due to the high-pass filtering, while the reflectance after this filtering should still be very close to the original reflectance. The reflectance can be also found by dividing the image by the low pass version if the original image, which is representing illumination components. Land proposed a technique called retinex, which is a combination of the words retina and cortex. The most interesting point for illumination normalization is the assumption that perception depends on the relative or surrounding illumination. It means that reflectance R(x, y) equals the quotient of image I(x, y) and the illumination L(x, y) calculated by the neighborhood of I(x, y). It improves the visibility of dark object while maintaining the visual different of the light area. Single scale retinex (SSR) algorithm proposed by

Pre-print of published paper:
To cite this article: Tajeripour, F., & Fekri-Ershad, S. (2014). Developing a novel approach for stone porosity computing using modified local binary patterns and single scale retinex. *Arabian Journal for Science and Engineering, 39*(2), 875-889.
DOI 10.1007/s13369-013-0725-8

Jobson et al [30] defines a Gaussian kernel to estimate the neighborhood illumination. Additional the logarithmic transformation is employed to compress the dynamic range. Reflectance image is computed by using Eq.19.

$$\mathbf{SSR(x, y)} = \log I(x, y) - \log [F(x, y) * I(x, y)] \quad (19)$$

Where, (*) denotes the convolution operation and F(x, y) is the surrounding Gaussian function. An example of normalized image based on SSR is shown in Fig.6
SSR technique has a high power to normalize and enhance the images, so it has been used for image normalization in different cases such as face recognition [31] and image enhancement [32]. SSR can be used to normalize the stone images according to the following stages:

I) All of the train and test images are normalized based on SSR

II) Proposed approach is applied on the normalized images

Results shows that using a preprocess image normalization stage based on SSR can improve the detection rate of proposed approach for porosity detecting.

(a) (b)
Figure(6). (a) Original Image (b) Normalized image based on SSR

In most of the inspection systems, the light source location, shine orientation, camera set and etc, are not the same. So, the captured images are different in contrast, brightness and illumination. Regarding to this problems, a preprocessing step like image normalization is necessary.
So far, many various techniques have been proposed for normalizing images, Such as gamma intensity correction [33], Block based histogram equalization [34], Homomorphic filtering [35], Adaptive histogram equalization [36] and etc. According to the following reasons, SSR technique is used for image normalization:

I) In the training stage of the proposed approach, LBP is applied on the whole image. Also, Single Scale Retinx normalizes the illumination in the whole image. So, by using SSR, the basic feature vectors which are extracted from the porosity-less images have more accurate values.

II) According to the section (6), the object information is included in reflectance, so the porosity areas are included in the reflectance. Also, output of single scale retinex is reflectance component of the original image. In this respect, normalizing the image by SSR, may improve the similarity between feature vectors that are extracted from porous windows.

III) According to the section (2), the Local Binary Patterns describes local contrast of an image. Also, single scale retinex normalizes the contrast. So, using SSR may increase the performance of LBP operator.

7. Results

In this paper, an approach was proposed for detecting the porosities in the architectonic stones. In order to evaluate performance of the proposed approach, first 60 images were taken from 3 kinds of architectonic stones called "Wave-less Cream Travertine", "Hatchet" and "Orange Travertine". These images were taken by a digital camera with the resolution of 0.2 mm/pixel. Also, for each kinds of stones just one image were taken from porosity-less stone for training stage.
Detection rate is one of the popular criteria for measuring the performance of defect detection approaches [28 and 37]. It is shown in Eq.20. So, the proposed approach was applied on the images and the detection rate was measured for each defect pattern. The average of detection rates is shown

Pre-print of published paper:
To cite this article: Tajeripour, F., & Fekri-Ershad, S. (2014). Developing a novel approach for stone porosity computing using modified local binary patterns and single scale retinex. *Arabian Journal for Science and Engineering, 39*(2), 875-889.
DOI 10.1007/s13369-013-0725-8

in the second row of table (2). To apply the proposed approach, different sizes were tested for windowing, and the sizes 16×16 provided maximum detection rate.

$$\textbf{Detection Rate} = 100 \times \frac{N_{cc} + N_{dd}}{N_{total}} \qquad (20)$$

In Eq.20, N_{cc} means the number of windows that were really porous and also were detected as porous window by the proposed approach. N_{dd} means the number of windows which were really porosity-less and also were detected as porosity-less window. To measuring the detection rate, the defect pattern was divided to non-overlap windows by the sizes of 16×16 pixels. After that, each window that has at least one defected pixel was counted as a porous window.
For example, in Fig.7 the first window (first column and first row) is categorized as porous window.

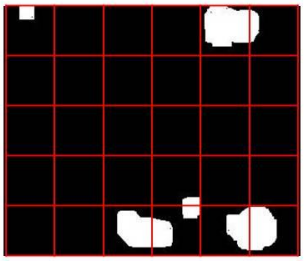

Figure (7). Determining result by defect detected image

The sensitivity (Eq.21) and specificity (Eq.22) were measured for all of the defect patterns. Average of these is shown in the second and third rows of the table (2).

$$\textbf{Sensitivity} = \frac{TP}{TP+FN} \qquad (21) \qquad \textbf{Specificity} = \frac{TN}{TN+FP} \qquad (22)$$

Where, TP, TN, FP and FN means true positive, true negative, false positive and false negative.

Table2. The detection rate, Specificity and Sensitivity of applying proposed approach on database

Stone / Criteria	Creamy Travertine	Hatchet	Orange Travertine
Detection Accuracy	**95,60**	**96.22**	**95.74**
Sensitivity	93.58	94.37	93.95
Specificity	96.76	96.66	96.81

In order to compare the performance of two dimensional LBP and one dimensional LBP, two dimensional LBP was applied on all of the database images. After that, detection rate, sensitivity and specificity were measured for all of the defect patterns. Averages of these are shown in tables (3, 4 and 5). For applying the two dimensional LBP, different neighborhoods sizes of neighbors (3×3, 5×5 and 7×7) were used. Some of the visual results are shown in Fig.8.

Table3. The average of detection rate of applying two dimensional LBP on database

Features	Stone / LBP Operator	Creamy Travertine	Hatchet	Orange Travertine
10	8,3	88,68	91.64	90.02
18	16,5	**93,67**	92.27	94.43
26	24,7	90.05	91.32	**95.43**
10 + 18	8,3 + 16,5	93.22	90.53	91.14
10 + 26	8,3 + 24,7	89.60	89.03	90.75
18 + 26	16,5 + 24,7	89.44	**94.11**	92.46
10 + 18 + 26	8,3 + 16,5 + 24,7	85.54	87.73	91.37

Pre-print of published paper:
To cite this article: Tajeripour, F., & Fekri-Ershad, S. (2014). Developing a novel approach for stone porosity computing using modified local binary patterns and single scale retinex. *Arabian Journal for Science and Engineering*, *39*(2), 875-889.
DOI 10.1007/s13369-013-0725-8

Table4. The average of sensitivity rate of applying two dimensional LBP on database

Features	Stone / LBP Operator	Creamy Travertine	Hatchet	Orange Travertine
10	8,3	85,98	90.40	89.45
18	16,5	**92,24**	91.83	93.31
26	24,7	89.32	90.29	**93.26**
10 + 18	8,3 + 16,5	91.84	87.72	89.31
10 + 26	8,3 + 24,7	87.60	88.20	89.66
18 + 26	16,5 + 24,7	89.24	**92.91**	90.66
10 + 18 + 26	8,3 + 16,5 + 24,7	83.32	86.40	91.03

Table5. The average of specificity of applying two dimensional LBP on database

Features	Stone / LBP Operator	Creamy Travertine	Hatchet	Orange Travertine
10	8,3	89,21	92.24	90.33
18	16,5	**94,02**	92.71	94.82
26	24,7	90.42	92.81	**95.89**
10 + 18	8,3 + 16,5	93.60	91.01	91.77
10 + 26	8,3 + 24,7	90.53	90.77	91.03
18 + 26	16,5 + 24,7	90.75	**95.42**	92.92
10 + 18 + 26	8,3 + 16,5 + 24,7	87.40	88.22	92.09

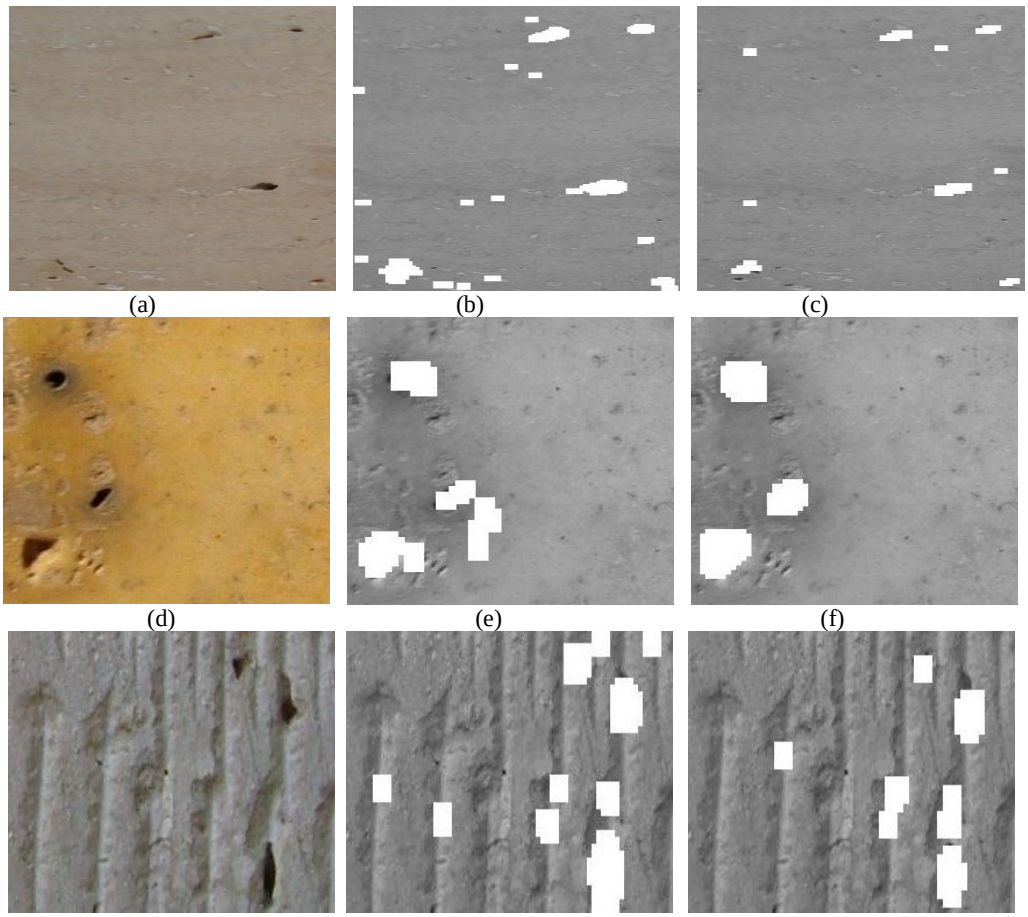

Pre-print of published paper:
To cite this article: Tajeripour, F., & Fekri-Ershad, S. (2014). Developing a novel approach for stone porosity computing using modified local binary patterns and single scale retinex. *Arabian Journal for Science and Engineering, 39*(2), 875-889.
DOI 10.1007/s13369-013-0725-8

(g) (h) (i)

Figure8. (a) Original Image of Creamy non-wavy travertine stone (b) defect detected of (a) by LBP 7×7 (c) defect detected of (a) by One dimensional LBP with L=8
(d) Original Image of Orange travertine stone (e) defect detected of (d) by LBP 3×3 & 7×7 (f) defect detected of (d) by One dimensional LBP with L=8
(g) Original Image of Hatchet stone (h) defect detected of (g) by LBP 5×5 (i) defect detected of (g) by One dimensional LBP with L=8

7.1. Results after normalization

In section (6), Single Scale Retinex was proposed to normalize training and testing images. So, in this section, first of all, the database images were normalized by SSR and then the proposed approach was used to detect porosity. The results are shown in table (6). The results show that the detection rate has been increased by using a preprocessing stage. Some of the defect patterns after using SSR are shown in Fig.9.

Table6. The detection accuracy, sensitivity and specificity of database after applying SSR

Stone / Rate Measure	Creamy Travertine	Hatchet	Orange Travertine
Detection Accuracy	**97,33**	**98.06**	**95.82**
Sensitivity	95.21	97.03	94.65
Specificity	98.66	98.82	97.23

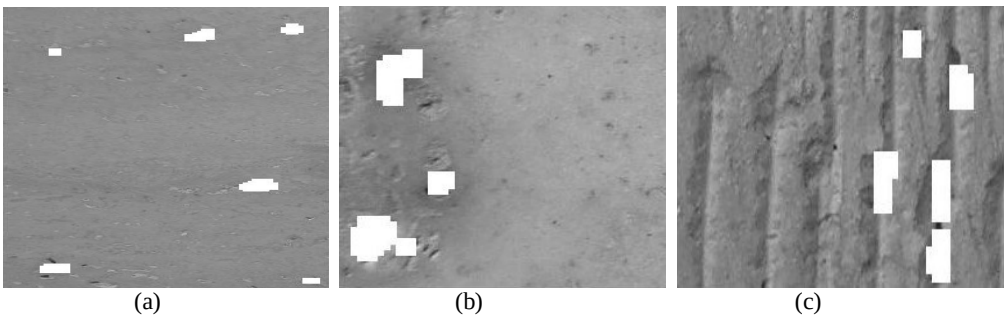

(a) (b) (c)

Figure (9). Some of the results after applying SSR
(a) Defect detection of fig (8).(a) after SSR
(b) Defect detection of fig (9).(d) after SSR
(c) Defect detection of fig (9).(g) after SSR

8. Stone Quality Categorization

Regarding the introduction part, porosity amount is one of the basic factors for categorizing the stone quality in stonecutting factories. In this paper, an approach was offered in order to detect the porosity in the architectonic stones. Now, the Eq.23 could be used to compute the porosity amount in the defect pattern. (output of the proposed approach).

$$\text{Porosity Amount} = \frac{D.D}{(m * n)} * 100 \qquad (23)$$

In Eq.23, D means the number of pixels that is declared as the porosity. Also, n and m are the image sizes. Civil engineers categorize the stones to five different grades based on their porosity amount. The first group has got the highest quality and the fifth is the lowest. It is shown in table (7) for 3 kinds of stones.

Table7. The quality categorization for database stones

Kind of Stone / Quality Degree	**Creamy Travertine**	**Hatchet**	**Orange Travertine**

Pre-print of published paper:
To cite this article: Tajeripour, F., & Fekri-Ershad, S. (2014). Developing a novel approach for stone porosity computing using modified local binary patterns and single scale retinex. *Arabian Journal for Science and Engineering, 39*(2), 875-889.
DOI 10.1007/s13369-013-0725-8

Grade 1	0 % - 5 %	0 % - 7 %	0 % - 3 %
Grade 2	5 % - 10 %	7 % - 14 %	3 %- 6 %
Grade 3	10 % - 15 %	14 %-21 %	6 % - 9 %
Grade 4	15 % - 20 %	21 % - 28 %	9 % - 12 %
Grade 5	20 % - 25 %	28 %- 35 %	12 % - 15 %

In table (7), each column shows one kinds of stones and every row shows the range of the porosity amount. So, after computing porosity amount, the stone quality can be categorized by using table (8). For example, in the table (8), the porosity amounts of stones in Fig.8 have been computed and they have been categorized.

Table8. Porosity amount determining on figure (8) images

Kind of Stone / LBP operator	Creamy Travertine	Hatchet	Orange Travertine
Two dimensional	2.84 % (grade 1)	5.45 % (grade 1)	3.76 % (grade 2)
One dimensional	1.25 % (grade 1)	3.45 % (grade 1)	3.47 % (grade 2)

According to the introduction part, stone quality categorization is done by experts now, which burden factories with much cost. Using this approach, Stone quality categorization in stonecutting factories can be done online more accurate, less expensive. To survey the performance of the proposed approach for stone quality categorization, all of the 60 images were categorized by the proposed approach once, and then, they were categorized by a human expert in civil engineering. The results taken showed that 96.66 % of the images were categorized correctly.

9. Conclusion

The main aim of this paper was to propose an accurate and fast approach for detecting and computing the porosity amount in architectonic stones. In this respect, a novel approach is proposed based on one dimensional local binary patterns and single scale retinex. The experimental results have showed that the proposed approach has a high detection rate for all kind of stones. Some other advantages of this approach are as follows:

I) one dimensional local binary pattern that proposed in this paper has less computational complexity than two dimensional local binary patterns.

II) The proposed approach has low sensitivity to noise as a result of windowing technique and considering the relation between each pixel and its neighbors

III) The proposed approach is a general one for two class classification problems. So it can be used for other defect detection cases

IV) In this paper, a novel feature vector is described that can be used for other image processing cases to analyze the textures.

V) High detection rate of the proposed approach compared with two dimensional local binary patterns operator shows the suitability of proposed approach with other feature operators.

VI) The proposed approach is a multi scale method. So, the results of choosing the different size of segments can be mixed by using the following equations, and it can be used for detecting the abnormalities in the stones. In eq(24 and 25), Z is the number of segments different sizes and K corresponds to the K_{th} windows.

$$L_{xK}^{Z} = \sum_{z=1}^{Z} L_{xK}(R_{xK}^{z}, M_{x}^{z}) \qquad (24)$$

$$L_{yK}^{Z} = \sum_{z=1}^{Z} L_{xK}(R_{yK}^{z}, M_{y}^{z}) \qquad (25)$$

VII) Accurate Computing porosity amount and online ability are unique advantages of proposed approach comparing other defect detection methods.

Acknowledgment:

The Authors would like to say thanks to Mr. Mohammad Abdollahi (Master Graduated of Civil engineering of Amirkabir University) and Mrs. Sepideh Fekri Ershad (Master Graduated of Civil

Pre-print of published paper:
To cite this article: Tajeripour, F., & Fekri-Ershad, S. (2014). Developing a novel approach for stone porosity computing using modified local binary patterns and single scale retinex. *Arabian Journal for Science and Engineering, 39*(2), 875-889.

DOI 10.1007/s13369-013-0725-8

engineering of Amirkabir University) for their guidance to collate the database and civil related descriptions.

References:

[1] Z. Zhaoa, N. Yeb, "Effective Semi-Supervised Nonlinear Dimensionality Reduction for Wood Defects Recognition", International Journal of Computer Science and Information Systems, **7** (2010), pp. 127-138.
[2] G.M.A. Rahaman and M. Hossain, "Automatic Defect Detection and Classification Technique from Image: a special case using ceramic tiles", International Journal of Computer Science and Information Security, **1(1)**(2009), pp. 22-30.
[3] W.P.Amorim, H.Pistori, M.C.Pereira, and M.A.C.Jacinto, "Attributes Reduction Applied to Leather Defects Classification", In Proc of 23rd SIBGRAPI Conference on Graphics, Patterns and Images, **1**(2010), pp. 353-359.
[4] A.Ghosh, T.Guha, R.B.Bhar, and S.Das, "Pattern Classification of Fabric Defects Using Support Vector Machine", International Journal of Clothing Science and Technology, **23(2-3)**(2011), pp. 142-151.
[5] P.N. Sargunar, R. Sukanesh, "Automatic Detection of Porosity and Slag Inclusion in Boilers Using Statistical Pattern Recognition Techniques", International Journal of Computer Applications, **1(21)**(2010), pp. 71-76.
[6] X. Xie, "A Review of Recent Advances in Surface Defect Detection using Texture analysis", Electronic Letters on Computer Vision and Image Analysis, **7(3)**(2008), pp. 1-22.
[7] C. Kim and A. Koivo. "Hierarchical Classification of Surface Defects on Dusty Wood Boards", Pattern Recognition Letters, **15(7)**(1994), pp. 713–721.
[8] R. Conners, C. McMillan, K. Lin, and R. Vasquez-Espinosa, "Identifying and Locating Surface Defects in Wood: Part of an automated timber processing system", IEEE Transactions on Pattern Analysis and Machine Intelligence, **5**(1983), pp. 573–583.
[9] H.Zhou, R.Wang and Ch.Wang, "A novel extended local binary pattern operator for texture analysis", Information Sciences, **178(22)**(2008), pp. 4314-4325.
[10] B.V.R.Reddy, M.R.Mani, B.Sujatha, and V.V.Kumar, "Texture Classification Based on Random Threshold Vector Technique", International Journal of Multimedia and Ubiquitous Engineering, **5(1)**(2010), pp. 53-62.
[11] H.G. Bu, X.B. Huang, J. Wang, X. Chen, "Detection of Fabric Defects by Auto-Regressive Spectral Analysis and Support Vector Data Description", Textile Research Journal, **80(7)**(2010), pp. 579-589.
[12] F.Lopez, F.Acebron, J.Valiente, and E.Perez, "A study of registration methods for ceramic tile inspection purposes", In Proc. of the IX Spanish Symposium on Pattern Recognition and Image Analysis, **1**(2001), pp. 145–150.
[13] A.Suresh, U.S.N. Raju and V. Vijaya Kumar, "An Innovative Technique of Stone Texture Classification Based on Primitive Pattern Units", International Journal of Signal and Image Processing, **1(1)**(2010), pp. 40-45.
[14] W.Wen and A. Xia, "Verifying Edges for Visual Inspection Purposes", Pattern Recognition Letters, **20**(1999), pp. 315–328.
[15] J.Chen and A.Jain, "A Structural Approach to Identify Defects in Textured Images", In Proc. of IEEE International Conference on Systems, Man, and Cybernetics, **1**(1988), pp. 29–32.
[16] K.L. Mak, P. Penga and K.F.C. Yiua, "Fabric Defect Detection using Morphological Filters", Elsevier Journal on Image and Vision Computing, **27**(2009), pp. 1585-1592.
[17] A.Monadjemi, M.Mirmehdi, and B.Thomas, "Restructured eigenfilter matching for novelty detection in random textures", In British Machine Vision Conference, **1**(2004), pp. 637–646.
[18] L.Latif-Amet, A.Ertuzun, and A.Ercil, "An efficient method for texture defect detection Sub-band domain co-occurrence matrices", Image and Vision Computing, **18(6-7)**(2000), pp. 543–553.
[19] D.Tsai, C.Lin, and K.Huang, "Defect detection in coloured texture surfaces using Gabor filters", Imaging Science Journal, **53(1)**(2005), pp. 27–37.
[20] H.G. Bua,, J. Wanga, and X.Huanga, "Fabric Defect Detection based on Multiple Fractal Features and Support Vector data Description", Elsevier Journal on Engineering Applications of Artificial Intelligence, **22(2)**(2009), pp. 224-235.
[21] F. Cohen, Z. Fan, and S. Attali, "Automated Inspection of Textile Fabrics using textural models", IEEE Trans. on Pattern Analysis and Machine Intelligence, **13(8)**(1991), pp. 803–809.
[22] X.Xianghua and M.Mirmehdi, "TEXEMS: Texture Exemplars for Defect Detection on Random Textured Surfaces ", IEEE Transactions on Pattern Analysis and Machine Intelligence, **29(8)**(2007), pp.1454-1464.
[23] K.Wooyoung and J.M.Rehg, "Detection of Unnatural Movement Using Epitomic Analysis", In proc. of seventh International Conference on Machine Learning and Applications(ICMLA), **1**(2008) , pp. 271-276.
[24] J.Mao and A.Jain, "Texture Classification and Segmentation using Multi resolution Simultaneous Autoregressive Models", Pattern Recognition, **25(2)**(1992), pp.173–188.

Pre-print of published paper:
To cite this article: Tajeripour, F., & Fekri-Ershad, S. (2014). Developing a novel approach for stone porosity computing using modified local binary patterns and single scale retinex. *Arabian Journal for Science and Engineering, 39*(2), 875-889.

DOI 10.1007/s13369-013-0725-8

[25] T. Maeenpaeae, M. Pietikaeinen, and T. Ojala, "Texture Classification by Multi Predicate Local Binary Pattern Operators", In Proc. 15th International Conference on Pattern Recognition, vol. 3, pp. 951-954, 2000.
[26] M.Pietikäinen, T.Ojala, and Z.Xu, "Rotation-Invariant Texture Classification Using Feature Distributions", Pattern Recognition, **33**(2000)**,** pp 43-52.
[27] T. Ojala, M. Pietikainen, and T. Maenpaa, "Multi resolution gray-scale and rotation invariant texture classification with local binary patterns", IEEE Transactions on Pattern Analysis and Machine Intelligence, **24(7)**(2002), pp. 971–987.
[28] F. Tajeripour, E. Kabir, and A.Sheikhi, "Fabric Defect detection using Modified Local Binary Patterns", EURASIP Journal on Advances in Signal Processing, **1**(2008), pp. 1-12.
[29] E. Land and J. McCann, "Lightiness and retinex theory", International Journal of Opt. Soc. America, **61**(1971), pp. 1–11.
[30] D. J. Jobson, Z. Rahman, and G. A. Woodell, "Properties and performance of a center/surround retinex", IEEE Trans. Image Process, **6(3)**(1997), pp. 451–462.
[31] Mariusz Leszczyński, "Image Preprocessing for Illumination Invariant Face Verification", Journal of telecommunications and information technology, **4**(2010), pp.19-25.
[32] D.H.Choi, I.H.Jang, M.H.Kim, and N.Ch.Kim, "Color image enhancement using single-scale retinex based on an improved image formation model ", In Proc. of 16th European Signal Processing Conference, Lausanne, Switzerland, **1**(2008)
[33] R.C.Gonzales, and R.E.Woods, "Digital Image Processing, Second Edition", Pearson Education International, Upper Saddle River, New Jersey, (2002).
[34] Xu.Xie and K.M.Lam, "Face Recognition under Varying Illumination Based on 2D Face Shape Model", Pattern Recognition, **38**(2005), pp. 221-230.
[35] R.Gonzalez and R.Woods, "Digital Image processing ", 2nd edition. Boston: Addison-Wesley Longman, (1992).
[36] S.MPizer and E.PAmburn, "Adaptive Histogram Equalization and its Variations", Computer Vision Graphics, Image Process, **39**(1987), pp. 355-368.
[37] A.Bodnarova, M.Bennamoun, and K.Kubik, "Suitability Analysis of Techniques for Flaw Detection in Textiles using Texture Analysis", Pattern Analysis & Applications, **3**(2000), pp. 254-266.